Study on spiral winding swimming motion control of a slender legless creature model[①]

Lu Zhenli (卢振利)[②][*], Ma Zhipeng[**], Marko Penčić[***], Maja Cavic[***], Borovac Branislav[***], Roumiana Ilieva[****], Bojan Nemec[*****], Marjan Mernik[******]

([*] School of Electrical Engineering and Automation, Changshu Institute of Technology, Changshu 215500, P. R. China)
([**] School of Information and Control Engineering, China University of Mining and Technology, Xuzhou 221116, P. R. China)
([***] Faculty of Technical Sciences, University of Novi Sad, Novi Sad 621000, Serbia)
([****] Faculty of Management, Technical University of Sofia, Sofia 1000, Bulgaria)
([*****] Department of Automatics, Biocybernetics and Robotics, Jožef Stefan Institute, Ljubljana 1000, Slovenia)
([******] Faculty of Electrical Engineering and Computer Science, University of Maribor, Maribor 462000, Slovenia)

Abstract

Through the observation and analysis of the motion trajectory of spiral winding motion for slender legless biological creatures in water, V-REP software is adopted to build a dynamic simulator to study on the mechanism of spiral winding swimming (SWS) motion. By using the output of spiral function(SF), the dynamic simulation model of slender legless creature (SLC) realizes the SWS motion in water. The corresponding experiments under the control of different bending angle of SF to control the dynamic model are also carried out to analyze the water performance of SWS in still water. Combined with the output of two different bending angles of the spiral function, the dynamic model can be used to realize SWS and up/down motion. This work provides technical reserve and experimental platform for the corresponding study in related fields.

Key words: V-REP, spiral winding swimming (SWS), motion control, slender legless creature (SLC)

0 Introduction

Spiral motion is a kind of constant motion form and phenomenon in nature. For example, in summer, a whirlwind in the field is a very intuitive spiral motion. The spiral motion in the magnetic field is more vibrating and oscillating. These oscillation and wave phenomena are often related to different physical motion functions. It is an abstract drawing that draws wave curve, spiral curve and various circulation lines with mathematical models of different parameters.

Spiral motion can be a form of dynamic motion for creature in liquid environments. Based on the spiral motion of slender legless creature (SLC) in a liquid environment, some simulation experiments are carried out to study the mechanism of spiral motion and to analyze its movement performance. This work can provide the platform and technical reserves for the study of spiral motion of slender legless bionic snakes and other creatures in water.

1 Related work

Most researches are related to spiral motion performance analysis of slender legless biological creatures in liquid, such as the analyses of the bionic mechanism from aspects, bacteria and sea snakes.

Most bacteria rely on spiral motion to move in the environment. Ref. [1] studied the motion of the caulobacter through tracking technology. The results show that its body seems to move along an invisible spiral tube track, which provides the motive force for limbless microorganisms to move around. Based on the mathematical model of 'resistance theory', the researchers demonstrated that the thrust of different bacteria can lead to different movements. For bacteria, spiral motion is an effective form of motion, and it is found that the speed of forward motion is faster than backward motion.

As shown in Fig. 1, some bacteria (e.g. spirobacteria) can show unique spiral (body spiral) move-

ments. In addition to crawling or creep buckling on the solid surface, these organisms can also adjust the axial fibers around the object to achieve their functions. The chemical composition of axonemes is very similar to flagella, but they are wrapped in spirochetes rather than in vitro.
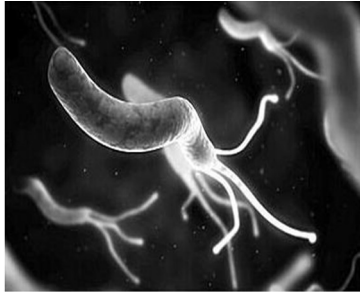

Fig. 1   Helix bacilli

Spiral movement can help sea snakes and sea otters to swim up and down in the ocean, as shown in Fig. 2. As for the bionic underwater snake-like robot, the spiral motion is considered to be a new motion for a wide range of application fields. A series of studies on the spiral climbing of snake-shaped robots for bridge cable climbing are conducted in recent years[2-5], which is for demonstrating the practicality of spiral motion in cable testing. The 3D underwater motion control of a snake-like robot is developed in simulation[6-7], and the three-dimensional motion gait of snake-shaped robots, the S-shaped tumbling and spiral tumbling of a real snake-like robot in water[8] are systematically studied. More researchers studied the mechanism design of snake-shaped robots, as well as their different applications[9-11].

Fig. 2   Sea snakes swimming

2   Development of SLC model in V-REP

2.1   SLC model

V-REP is adopted as simulation platform to study the helical motion of SLC model. In V-REP simulation platform, cylinder is selected as the main spiral motion model of module. The type of joint is revolute with the dynamic properties of the force/torque model, so as to program to drive to control the joint. Sphere is selected as a carrier of orthogonal joint, as shown in Fig. 3, where the vertical joints and horizontal joints are independent movement.
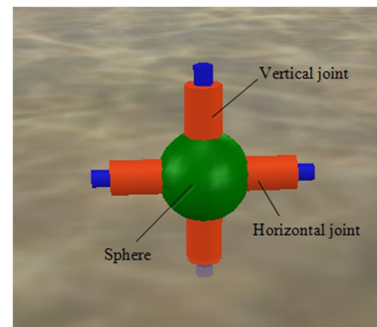

Fig. 3   Orthogonal joint

SLC model is developed with 9 modules for the study of spiral motion simulation, as shown in Fig. 4. In order to easily distinguish the motion direction, the outer edge of the head module is set to green, and another side is defined as tail. The dynamics parameters of the SLC model are shown in Table 1.
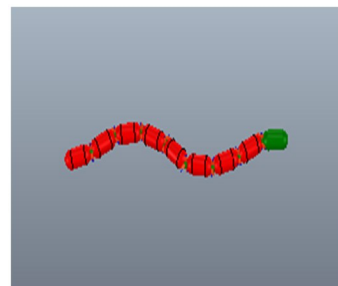

Fig. 4   SLC model

Table 1   Main parameters in the model

Number of joint	Weight /g	Diameter /mm	Length /mm	Moment /N · m
9	200	100	200	5

2.2   Define the water dynamic in V-REP

The spiral winding swimming (SWS) motion of the SLC model is carried out under the condition of still water, where the environment factors, such as water waves, water velocity, are not considered. In this work, mainly two kinds of force are control the simulation model to realize the SWS in the water. One group force is its own gravity and the buoyancy of water on the model, the other group is generated by SWS of SLC model where the water will produce interaction force between viscous drag[12-13].

The following forces will be analyzed for SWS of SLC model in still water.

(1) The gravity G_i of each link in SLC model

$$G_i = m_i g \qquad (1)$$

where, m_i is the mass of the i-th module, i refers to the module number, g is the gravitational acceleration.

(2) The buoyancy F_i of each link in SLC model

There is no actual surface in the simulation environment, so it is needed to call the SimAddForce function of the software to add a simulation model for the module, so that the reverse direction of gravity is similar to the buoyancy of the actual water environment. Considering that the buoyancy cannot be calculated directly according to the submerged volume, here in each module (perpendicular to the horizontal plane), the approximate position of the centroid of Z axis is relative to the horizontal plane ($Z = 0$) plus the buoyancy F_i.

$$F_i = \frac{50 - Z_i}{100} \cdot m_i g \quad Z_i \leqslant 50 \qquad (2)$$

In this system of the still water, if Z is less than -50, it can be determined by the approximate buoyancy.

(3) The simulation model of the viscous drag f

When the simulation model moves on the water, each module will be affected by the viscous resistance of the water. The viscous resistance model in X, Y, Z coordinate system is analyzed. The resistance is related to the velocity of the model. In the simulation, the V-REP resistance coefficient is set to a negative value, and the component resistances on the X, Y and Z axes are

$$\begin{cases} f_{i,x} = v_{i,x} \cdot m_i \cdot s_c \cdot c_i \\ f_{i,y} = v_{i,y} \cdot m_i \cdot s_c \cdot c_i \\ f_{i,z} = v_{i,z} \cdot m_i \cdot s_c \cdot c_i \end{cases} \qquad (3)$$

where, v_{ix}, v_{iy} and v_{iz} are the three velocity components of the module speed in the direction of axis x, y, z; s_c is viscous resistance coefficient which is determined by the fluid state and the surface roughness of the rigid body; m_i is the mass for each module; c_i depends on the height of mass center coordinates relative to the horizontal plane for each module.

3 Control function for SWS motion

In order to achieve the spiral motion control, the Serpenoid curve function proposed to synthesize snake shaped is adopted to generate rhythm of the rotation angle of each joint[14-16].

This function after extension can be used to control spiral motion of SLC model as shown in Fig. 5.

Serpentine curve curvature equation is shown as

$$\rho = -\alpha b \sin(bs) \qquad (4)$$

where, α is the initial amplitude curveting radian, b is the proportionality constant, s is the arc length of the serpentine curves.

$$\theta(s) = \alpha \cos(bs) \qquad (5)$$

where, $\theta(s)$ is the angle in the tangent direction along the serpentine curves arc length s.
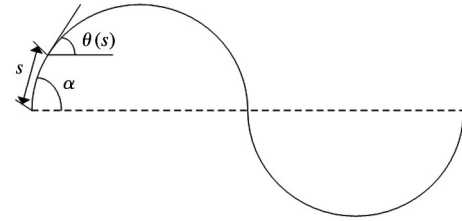

Fig. 5 Serpentine curve

According to Eq. (5), the joint angle φ for connecting adjacent joints of the SLC model is shown as

$$\varphi = \theta(s + l) - \theta(s - l) = -2\alpha \sin(bl)\sin(bs) \qquad (6)$$

where $2l$ is the length of the connecting rod of a single model.

According to Eq. (6) to control SLC model to generate the spiral motion, the discretization of the adjacent joints of the formula is shown as

$$rad[i] = (-2) \cdot \alpha \cdot \sin\left(\frac{kn \cdot \pi}{N}\right)$$
$$\cdot \sin\left(\frac{2 \cdot kn \cdot \pi \cdot S}{L} + \frac{2 \cdot kn \cdot \pi \cdot i}{N}\right) \qquad (7)$$

where, i is joint number of the SLC model, α is starting angle, kn is s-wave number in the body, S is displacement of the simulation model along the axis direction, L is the total length of model, N is the module number, $rad[i]$ is the corresponding i-th joint rotation angle in radian. The corresponding simulation model of each connecting rod module at a certain moment in the process of movement state is shown in Fig. 6.
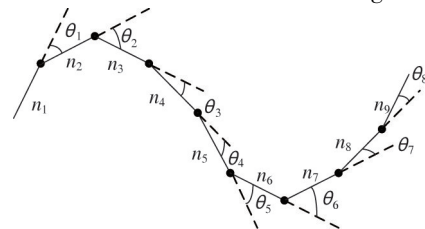

Fig. 6 Connecting rod swing state

In Fig. 6, n_1, n_2, $\cdots$, n_9 are respectively simulation model connecting rod module; θ_1, θ_2, $\cdots$, θ_8 are respectively the angle between the adjacent link module from head to tail; the serpentine curve is discrete by linkage mass m_i with fixed length $2l$.

SWS motion of SLC model in still water is realized by the rotation of the orthogonal connection joint mechanism, which is a kind of three-dimensional movement gait coupled by vertical and horizontal rotation. Its im-

plementation requires a combination of vertical joints and horizontal joints, which can be obtained from Eq. (7) with the following control function:

$$
\begin{cases}
\varphi_v[i] = (-2) \cdot \alpha_v \cdot \sin(\dfrac{kn \cdot \pi}{N}) \\
\qquad \cdot \sin(\dfrac{2 \cdot kn \cdot \pi \cdot S}{L} + \dfrac{2 \cdot kn \cdot \pi \cdot i}{N}) \\
\varphi_h[i] = (-2) \cdot \alpha_h \cdot \sin(\dfrac{kn \cdot \pi}{N}) \\
\qquad \cdot \cos(\dfrac{2 \cdot kn \cdot \pi \cdot S}{L} + \dfrac{2 \cdot kn \cdot \pi \cdot i}{N})
\end{cases}
$$

(8)

where, $\varphi_v[i]$ is the vertical deflection angle of the i-th joint, $\varphi_h[i]$ is the horizontal deflection angle of i-th joint, and the phase difference of curve function is $\pi/2$, α_v and α_h are starting angles of serpentine curves respectively applied to vertical joints and horizontal joints.

4   Performance analysis of SWS motion

4.1   Performance analysis of spiral shape

In terms of screw motion control function, the different combinations of initial angle α_v and α_h determine the configuration of initial state simulation model of screw motion and the size of screw radius.

The parameter kn in the control function determines the number of S waves in the SLC model, and also determines the number of spirals in the model. The change speed of parameter s determines the speed of spirals. α_v and α_h are set as the same values, the experiments are carried out under different screw configurations, as shown in Fig. 7.
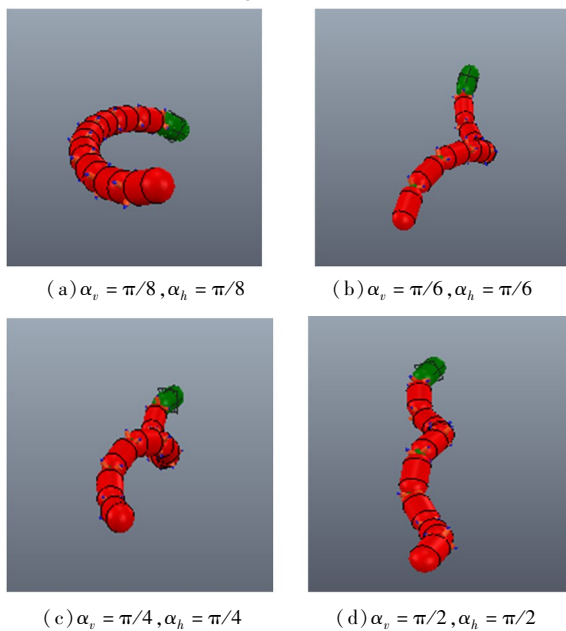

(a) $\alpha_v = \pi/8$, $\alpha_h = \pi/8$ (b) $\alpha_v = \pi/6$, $\alpha_h = \pi/6$

(c) $\alpha_v = \pi/4$, $\alpha_h = \pi/4$ (d) $\alpha_v = \pi/2$, $\alpha_h = \pi/2$

Fig. 7 α_v and α_h under different radius of a spiral

When α_v and α_h are set as different values, two kinds of situations are discussed. When $\alpha_v > \alpha_h$, SLC model will generate the spiral winding along the horizontal (X) direction. When the value of angle of α_h is set very small, the simulation model will generate a spiral winding motion alone the horizontal (X) direction. When $\alpha_v < \alpha_h$, the simulation model will generate the spiral winding along the vertical (Y) direction, the movement is also called the spiral dive up/down swimming. The experiments under different kn spiral coil number are shown in Fig. 8.
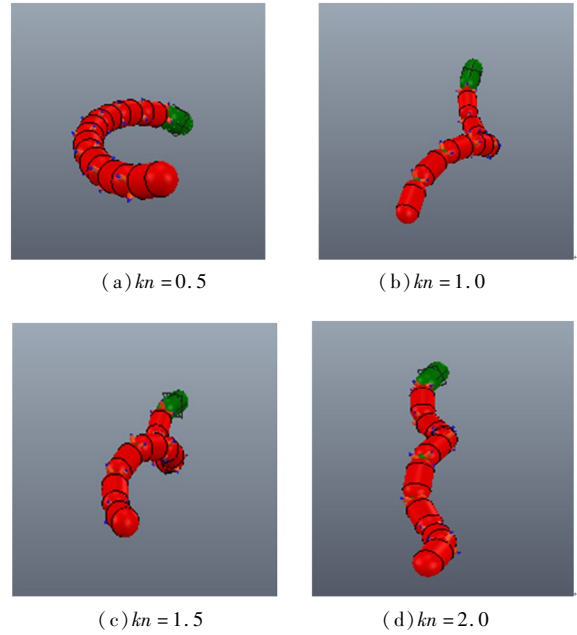

(a) $kn = 0.5$ (b) $kn = 1.0$

(c) $kn = 1.5$ (d) $kn = 2.0$

Fig. 8   Experimental results under different kn

4.2   Performance analysis of starting angle

In the control function, when different values of α_v and α_h are given, different screw models will be formed. Under the condition of spiral winding gait, given that α_v is equal to α_h, choose $\alpha_v = \pi/2$, $\alpha_h = \pi/2$ to carry out SWS experiment analysis, and the movement process is shown in Fig. 9.

In the spiral winding swimming process, according to the recorded torque information of the vertical and horizontal joints of SLC model, the simulation results are obtained, as shown in Fig. 10 and Fig. 11.

In the experiment of spiral winding swimming, according to the torque diagram in Fig. 10 and Fig. 11, in the vertical direction of the dynamic model, joint 4 and joint 5 need larger torque compared with other joints; in the horizontal direction, joint 4 and joint 5 need smaller torque compared with other joints. In the simulation model of spiral configuration, module 4 and module 5 are in two reverse spiral arc joints. In order to maintain the spiral configuration, the torque changes of joint 4 and joint 5 are different from other joints in

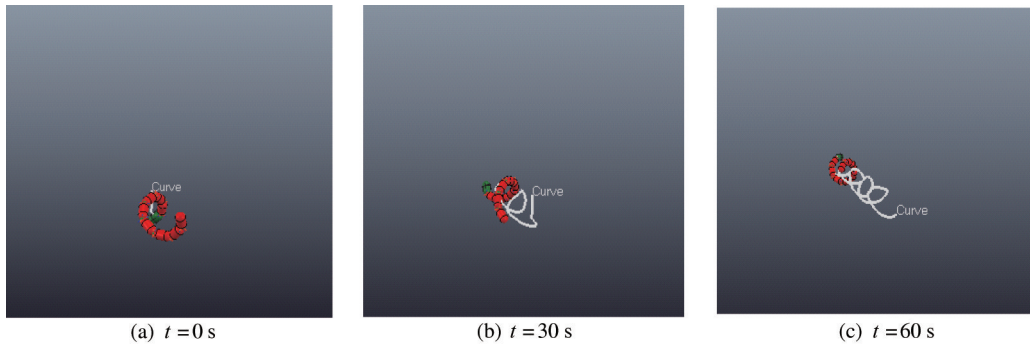the vertical and horizontal directions.

(a) $t = 0$ s   (b) $t = 30$ s   (c) $t = 60$ s

Fig. 9   SWS motion ($\alpha_v = \pi/2$, $\alpha_h = \pi/2$)
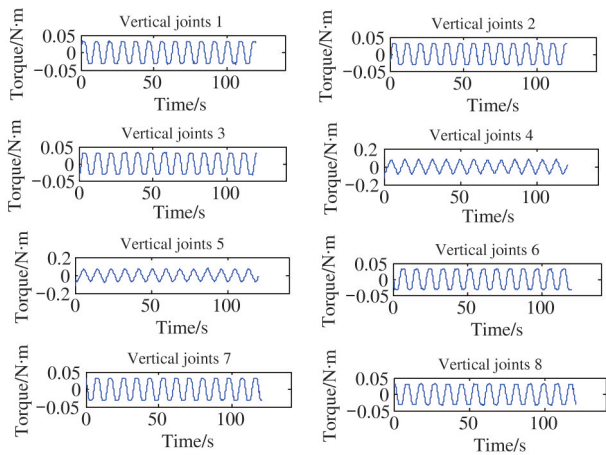
Fig. 10   Torque of the vertical joints

Fig. 12   2D trajectory of SWS

Fig. 11   Torque of the horizontal joints

Fig. 13   3D trajectory of SWS
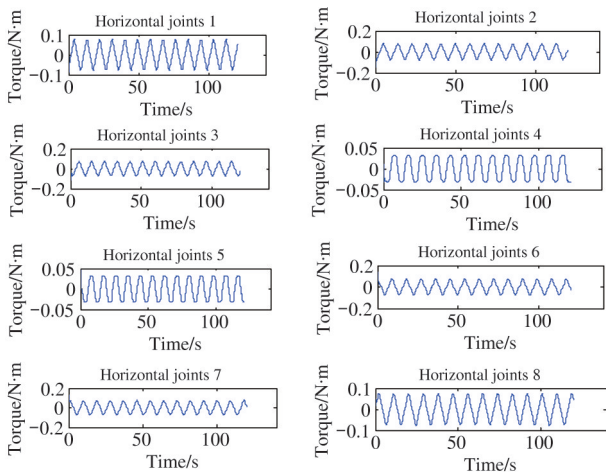
During the experiment, the head module center of mass of the dynamic model moves along the X and Y directions in the process of spiral winding, as shown in Fig. 12, basically in a straight line direction; meanwhile, the three-dimensional tracks of the model in the X, Y and Z directions are shown in Fig. 13.

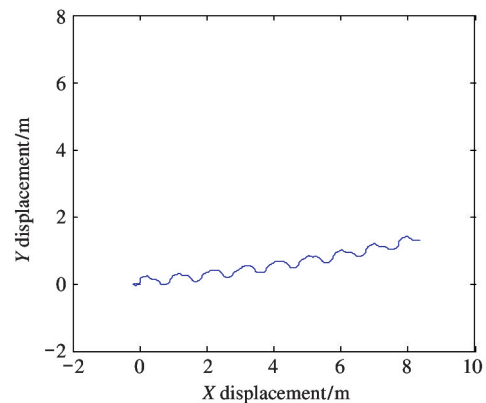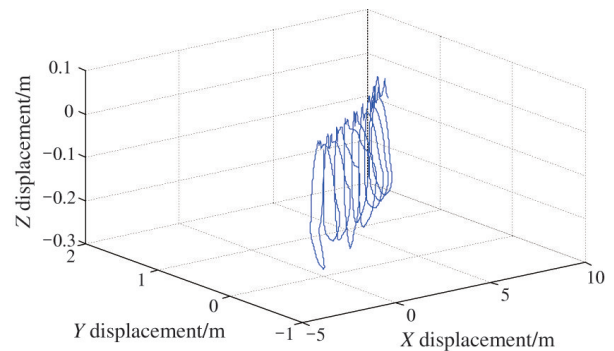It can be seen that the trajectory of SLC model under the driving excitation is a spiral roll with lateral resistance. Choose $\alpha_v = \alpha_h$, give different starting angle of helix to carry out the experiment, and the relationship between the spiral winding speed and the starting angle of helix can be obtained, as shown in Fig. 14.

The experimental results show that the smaller the initial helix angle is, the smaller the helix radius is, and the lower the helix velocity is. When the initial angle of the spiral is very small gradually, the simulation model can still slowly complete the small radius circular spiral action and move forward. From the point of view of energy consumption, the larger the start angle of the screw controlling the excitation input, the larger the spatial circumferential radius of the screw structure

of the SLC model, which will also lead to the greater the joint torque change and the increase of energy consumption.
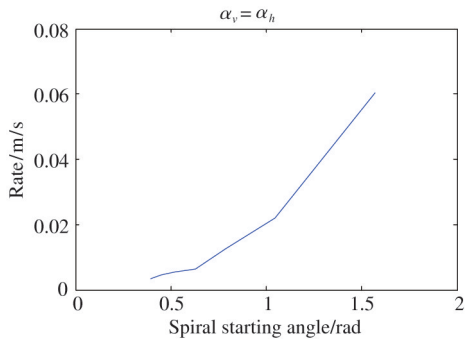

Fig. 14 $\alpha_v = \alpha_h$ for different spiral starting angles

In the simulation model of spiral winding, when $\alpha_v = \alpha_h$, it is like a circle helical screw configuration. When $\alpha_v \neq \alpha_h$, it is like oval ring spiral screw configuration. If we consider the application in water or on land for similar robots, for this kind of configuration, the simulation model of the helical winding can realize more given direction motion in water, such as spiral rise, and spiral dive in water. This kind of movement gait is not only unstable, but also difficult to control to switch from other movement gaits, such as serpentine locomotion on land and other applications[17-20]. The control method of spiral winding is more suitable for the application in water.

When $\alpha_v = \pi/2$, $\alpha_h = \pi/8$, spiral winding process is shown in Fig. 15. Its movement form embodies mainly the swimming along the vertical direction of spiral dive and buoyancy.
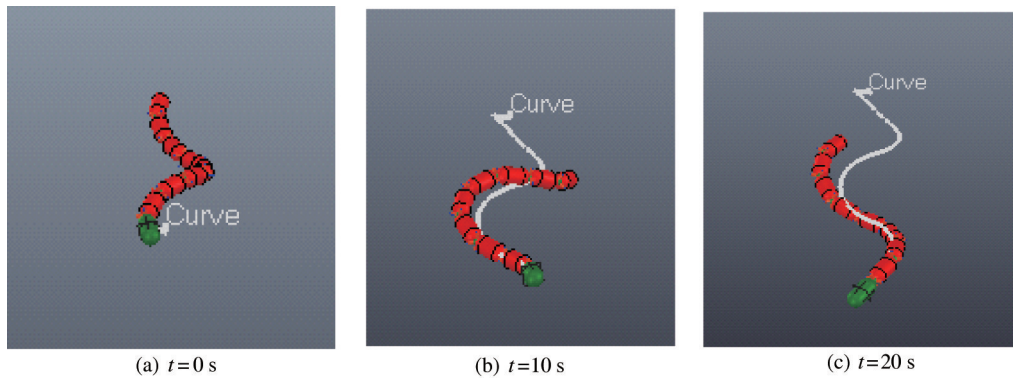

(a) $t = 0$ s   (b) $t = 10$ s   (c) $t = 20$ s

Fig. 15   Spiral winding process ($\alpha_v = \pi/2, \alpha_h = \pi/8$)

The experimental results of spiral winding, where $\alpha_v = \pi/8, \alpha_h = \pi/2$, are shown in Fig. 16, which is the forward movement of spiral winding along the horizontal direction.

According to the movement experiment results of the model given different initial angle input of spiral winding, it can be seen that due to the lack of suffi-cient water support force, when the vertical and horizontal initial angle of SWS is smaller, the movement effect of SWS is poorer, the efficiency is lower, and the rolling is carried out in situ. The simulation model can realize arbitrary coiling of space without considering the phenomenon of rollover. Its main disadvantages are uncontrollable direction and low efficiency.
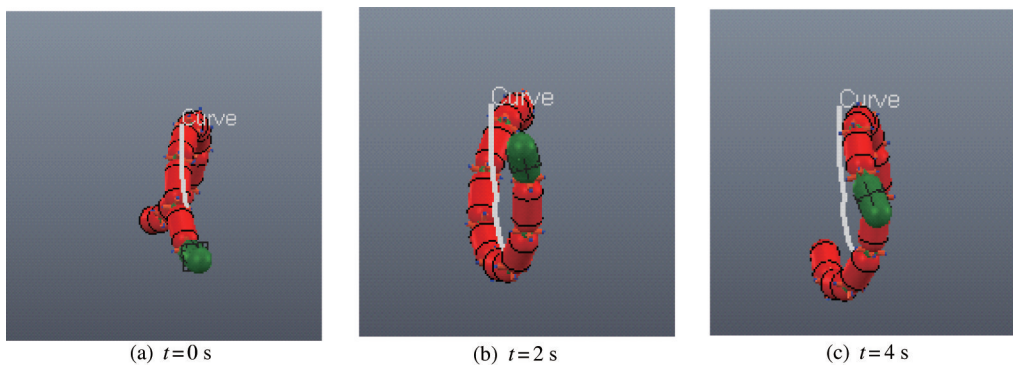

(a) $t = 0$ s   (b) $t = 2$ s   (c) $t = 4$ s

Fig. 16   Spiral winding process ($\alpha_v = \pi/8$, $\alpha_h = \pi/2$)

5   conclusions

Inspired by the spiral motions of different living creature and natural tornado phenomenon, a SWS motion of SLC in water is developed. Firstly, through the mechanism analysis, the spiral motion can be an effective motion of SLC in water. Secondly, the spiral helical radius and the body turns the morphology of spiral motion are analyzed with a math function output controlled the dynamic model of the legless creature. Thirdly, under different bending angle of spiral math function, the performance of SWS motion of the dynamic model is also analyzed. Finally, through changing the value of bending angle of the spiral function, the dynamic model of SLC can realize SWS together with the up and down function.

Reference

[1] Liu B, Gulino M, Morse M, et al. Helical motion of the cell body enhances caulobacter crescentus motility [J]. *Proceedings of the National Academy of Sciences*, 2014, 111(31), 11252-11256

[2] Wei W, Zhu H. Research of helical rolling gait of snake-like robot in detection of bridge cables[J]. *Computer Engineering and Design*, 2011, 32(2):700-702 (In Chinese)

[3] Endo G, Kawato M, Cheng G, et al. Robot and attitude control method of robot[P]. US Patent: US20050113973 A1, 2005

[4] Kulkarni A, Chawla R. Structure and analysis of a snake-like robot[C] // Innovative Algorithms and Techniques in Automation, Industrial Electronics and Telecommunications, Dordrecht, Netherlands, 2007: 43-47

[5] Wei W, Yu J, Lin W, et al. Structure design of climbing snake-like robot for detection of cable-stayed bridge[J]. *Applied Mechanics and Materials*, 2014, 598:610-618

[6] Tang J, Li B, Chang J, et al. Design and dynamic model of underwater gliding snake-like robot [J]. *Journal of Huazhong University of Science and Technology*, 2018,46 (12), 89-94 (In Chinese)

[7] Yang B, Han L, Li G, et al. A modular amphibious snake-like robot: design, modeling and simulation[C] // IEEE International Conference on Robotics and Biomimetics, Zhuhai, China, 2015: 1924-1929

[8] Yu S, Wang M, Ma S, et al. Development of an amphibious snake-like robot and its gaits on ground and in water [J]. *Journal of Mechanical Engineering*, 2012, 48(9): 18-25

[9] Yang B, Mu Z, Liu T, et al. Biomimetic snake robot in complex marine medical rescue application[J]. *Journal of Medical Imaging and Health Informatics*, 2018,8(2): 232-239

[10] Yaqub S, Ali A, Usman M, et al. A spiral curve gait design for a modular snake robot moving on a pipe[J]. *International Journal of Control Automation and Systems*, 2019, 17: 2565-2573

[11] Takemori T, Tanaka M, Matsuno F. Gait design for a snake robot by connecting curve segments and experimental demonstration [J]. *IEEE Transactions on Robotics*, 2018, 34(5):1384-1391

[12] Lv Y, Li L, Wang M, et al. Simulation study on serpentine locomotion of underwater snake-like robot[J]. *International Journal of Control and Automation*, 2015, 8 (1):373-384

[13] Zuo Z, Wang Z, Li B, et al. Serpentine locomotion of a snake-like robot in water environment[C] // IEEE International Conference on Robotics and Biomimetics, Bangkok, Thailand, 2009: 25-30

[14] Hirose S. Biologically Inspired Robots: Snake-like Locomotors and Manipulators[M]. England: Oxford University Press, 1993:351-363

[15] Sun H, Ma P, Wang G. An inchworm locomotion gait basedon serpenoid curve for snake-like robot [J]. *Mechanical Design and Research*, 2008, 24(1):39-41

[16] Ye C, Ma S, Li B, et al. Development of a three dimensional snake-like robot perambulator II[J]. *Journal of Mechanical Engineering*, 2005, 15(3):25-31 (In Chinese)

[17] Hopkins J, Gupta S. Design and modeling of a new drive system and exaggerated rectilinear-gait for a snake-inspired robot [J]. *Journal of Mechanisms and Robotics*, 2014, 6(2):1-8

[18] Hopkins J, Gupta S. Dynamics-based model for a new class of rectilinear-gait for a snake-inspired robot[C] // ASME International Design Engineering Technical Conferences and Computers and Information in Engineering Conference, Chicago, USA, 2012: 151-160

[19] Weng Z, Liu T, Wu C, et al. Mechanism design and kinematic performance research of snake-like robot with orthogonal active wheels[J]. *Advances in Reconfigurable Mechanisms and Robots II*, 2015, 36:603-615

[21] Manzoor S, Choi Y. Recurring side-winding motion generation for modular snake robot[C] //2017 IEEE International Conference on Robotics and Biomimetics (ROBIO), Macao, China, 2017: 1468-1473

Lu Zhenli, born in 1974. He received his Ph. D degree in Shenyang Institute of Automation, Chinese Academy of Sciences. His research interests include robot intelligent control, human robot interaction.